Technical Design Report for HADES-100

Investigation of Dilepton Production at SIS100 with HADES*

P. Finocchiaro[2], P. Fonte[8], J. Friese[10],V. Friese[4], R. Gernhäuser[10]
J. A. Garzón[1], F. Guber[9], C. Höhne[4], R. Holzmann[4],
B. Kämpfer[5], I. Koenig[4], W. Koenig[4], B. W.Kolb[4], R. Kotte[5],
R. Krücken[10], A. Kugler[12], A. Kurepin[9], J. Markert[7], W. Müller[4]
C. Müntz[7], L. Naumann[5], J. Pietraszko[4], W. Przygoda[3]
P. Salabura[3], P. Senger[4], J. Stroth[7,4],
P. Tlusty[12], M. Traxler[4], H. Tsertos[11], Y. Zanevsky[6]

[1] *Departamento de Física de Partículas, University of Santiago de Compostela, 15782 Santiago de Compostela, Spain*
[2] *Istituto Nazionale di Fisica Nucleare - Laboratori Nazionali del Sud, 95125 Catania, Italy*
[3] *Smoluchowski Institute of Physics, Jagiellonian University of Cracow, 30059 Cracow, Poland*
[4] *Gesellschaft für Schwerionenforschung mbH, 64291 Darmstadt,Germany*
[5] *Institut für Strahlenphysik, Forschungszentrum Dresden-Rossendorf, 01314 Dresden, Germany*
[6] *Joint Institute of Nuclear Research, 141980 Dubna, Russia*
[7] *Institut für Kernphysik, Johann Wolfgang Goethe-Universität, 60486 Frankfurt, Germany*
[8] *LIP-Laboratório de Instrumentação e Física Experimental de Partículas, 3004-516 Coimbra, Portugal*
[9] *Institute for Nuclear Research, Russian Academy of Science, 117312 Moscow, Russia*
[10] *Physik Department E12, Technische Universität München, 85748 Garching, Germany*
[11] *Department of Physics, University of Cyprus, 1678 Nicosia, Cyprus*
[12] *Nuclear Physics Institute, Academy of Sciences of Czech Republic, 25068 Rez, Czech Republic*

Abstract

This paper presents the concept of study electron-positron pair production in the beam-energy range of 2-10 AGeV by making use of the High-Acceptance Di-Electron Spectrometer (HADES), being now in operation at SIS18. The planned new FAIR facility will provide for the first time the opportunity to perform dielectron measurements by HADES at SIS100 in a hitherto completely unexplored range of beam energies, characterized by a substantially larger compression of nuclear matter. Our simulations of such a scenario show promising results in terms of achievable dilepton acceptance and resolution. Parasitically, hadrons are accessible, too, thus providing a link to the AGS energy range. The efforts to transport the spectrometer and install it at FAIR SIS100 involve only moderate costs and manpower.

* Corresponding author: phone: +49-6159-71 1632, fax: +49-6159-71 2989,
e-mail: j.pietraszko@gsi.de

1 Physics motivation

The study of nuclear matter properties at high densities and temperatures is one of the main objectives in relativistic heavy-ion physics. In this context, the paramount aim of probing dilepton radiation from the fireball is to extract in-medium mass distributions (spectral functions) of the light vector mesons (ρ, ω, ϕ). These spectral functions are expected to yield information on the restoration of the spontaneously broken chiral symmetry in hot and dense nuclear matter. During the evolution of the fireball the properties of nuclear matter change drastically and the dilepton spectrum, which is not hampered by final-state interactions, encodes information about all emission processes integrated over the whole collision history. With precise knowledge of particle yields at chemical freeze-out, obtained from hadronic observables, it is however possible to subtract the late contributions from the pair spectrum, revealing thus the "true" in-medium component. The ultimate goal is to achieve a full understanding of hadrons in matter under various conditions of temperature and density. Evidently, this goal can be reached only by combining results from complementary experiments scanning different parts of the nuclear matter phase diagram. Fig. 1 shows this diagram, together with the chemical freeze-out line determined within a statistical model [1], as well as those areas explored by past, existing and planned experiments. The mission

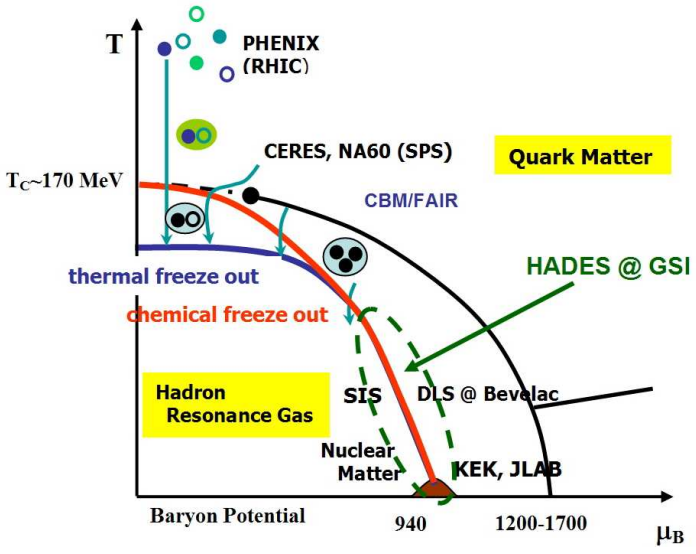

Fig. 1. Schematic sketch of the phase diagram of nuclear matter. Operating regimes of various dielectron experiments are depicted. The region accessible by HADES at SIS18 and SIS100 is indicated as dashed ellipse.

of HADES-100 at the future FAIR facility will be to provide high-quality dielectron data at baryon densities and temperatures not accessible by other

detectors, neither in the past nor in the foreseeable future. The dilepton opportunities of the Compressed Baryon Matter (CBM) experiment at SIS300 will later on continue the study of the dilepton emissivity of compressed nuclear matter at higher beam energies and bridges over to CERN energies.
At beam energies available from SIS18 (1-2 AGeV), one can investigate nuclear matter at temperatures of T = 40-90 MeV and baryon densities of 1-3 ρ_0. The systematic investigation of this region, including meson production in N+N, p+A and A+A collisions, is at the focus of the present HADES experimental programme. Based on the completed analysis of available data one can conclude [2,3] that the main source of dielectrons contributing to the in-medium radiation are decays of the short-lived baryonic resonances Δ, N^* and, at low energy, quasi-elastic p-n bremsstrahlung. The decay of these resonances also dominates the mass region of the vector mesons with important off-shell contributions. The role of light vector mesons is still to be clarified. This is very much different from the situation at SPS or RHIC energies, where pion annihilation via the rho resonance dominates the in-medium dilepton yield [4,5] in the region beyond the π^0-Dalitz region. On the other hand, the influence of baryons was found to be decisive for the explanation of the in-medium spectral function of the rho at SPS energies. These coupling effects are therefore expected to be very important at moderate beam energies where the fireball is dominated by baryons. Indeed, results obtained by CERES at 40 AGeV support, despite their poor statistics, this expectation.
At the beam energies of SIS100 at FAIR nuclear matter densities exceeding substantially those achievable at SIS18 can be reached. The temperatures are expected to remain below those estimated for the transition to the guark-gluon plasma. Exploring this region of the phase diagram is the main purpose of the proposed HADES programme at FAIR. One should note that, since between 2 and 40 AGeV no dilepton data exist so far, this is complete "terra incognita" for dielectron measurements. From the experimental point of view, the challenges in terms of particle rates and background are comparable to those faced already now at SIS18, with the present HADES set-up operating near the light vector-meson production thresholds. As the higher SIS100 energies lead to significantly enhanced production of vector mesons, the extension of the HADES physics programme to higher energies is a natural option.
Figure 2 shows meson multiplicities predicted with the statistical model [6]. Pion yields, used for the normalization, have been taken from existing experimental data. Thermodynamic parameters, like freeze-out baryon chemical potentials and temperatures, where fitted from available particle ratios [7] and are shown on the right side. Note that the chemical potential, which drops rapidly between 1 and 10 AGeV beam energies, approaches the low-energy SPS point. As one can see, the normalized vector-meson yields increase by two orders of magnitude when going from SIS18 to SIS100 bombarding energies, and saturates quickly at even higher energies. Guided by the results of the statistical hadronic model one can further try to infer the systematics of achievable baryon net densities by inspection of the corresponding freeze-

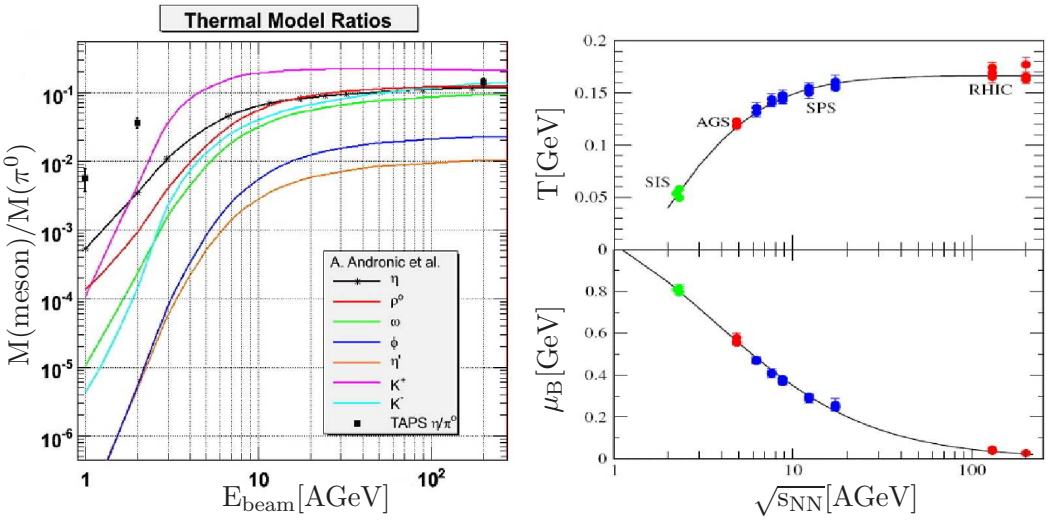

Fig. 2. Left: Prediction within the statistical model [6] of meson multiplicities, normalized to the pion yield, as a function of beam energy. Points indicated correspond to available data on eta-meson production. Right: Temperature and baryon chemical potential at freeze-out as a function of total center-of-mass energy per nucleon as obtained from statistical model fits [7] to data.

out densities: At kinetic beam energy of 10 AGeV the freeze-out density is $0.10/fm^3$ [8], being two times larger than that at SIS18. As rough estimate one my argue that also the density in the maximum compression stage is sizeably larger than at SIS18. At the same time, the model [9] points to a contribution of baryons to the total entropy density (also at freeze-out) being twice as large as that of mesons at kinetic beam energy of 10 AGeV. In this respect, at SIS100 we expect high baryon net densities with clear dominance of baryons. At larger beam energies (say from 20 - 40 AGeV) the net baryon freeze-out density saturates at maximum values around 0.13/fm^3, (i.e., being somewhat larger), but the meson contribution is as large (or even larger) as the baryon contribution. This means, at SIS100 the focus will be on baryon density effects, while SIS300 offers the avenue to maximum baryon density effects at the onset of meson dominated strongly interacting matter and will open an access to the predicted deconfinement phase transition. Clearly, this reasoning is based on the freeze-out condition for hadrons, but it may serve as some guidance for the compression stage, too, and the relevant degrees of freedom for the dielectron emissivity. In the work of Rapp and Wambach [10] on the in-medium rho-meson spectral function and related dielectron spectra much emphasis is put on the the distinction whether baryons or mesons drive the in-medium modification. In this respect, a step-by-step measurement of the corresponding excitation function of differential dielectron spectra appears as an essential experimental input.

The freeze-out energy densities at SIS100 go up to 150 MeV/fm^3. One might argue that the transport modeling of the course of the collision is not hampered

by conceptional problems. The interpretation of the expected data will rest, similar to the situation in other energy regimes, on such dynamical models.

HADES is a running installation with well-understood performance which allowed to achieve remarkable results [2,3]. The transfer to SIS100 will benefit from the high-level experience of the crew. In so far, we expect that HADES at SIS100 can immediately start to take physically relevant data and produce important results. The planned installation of HADES and CBM apparatuses in the cave foresees a completely independent operation of both experiments which will allow the HADES to take data till the operation of CBM at SIS300 and even perform experiments during the commissioning phase of the CBM experiment.

2 Physics performance study - simulation for HADES at 2-10 AGeV

In this section, simulations of the HADES performance in 8 AGeV A+A collisions are presented and compared with simulation results at 1 and 2 AGeV. The main effort was focused on getting the basic figures on the acceptance of HADES for systems available at FAIR. Cross sections of meson production in NN reactions in this energy range are only partially or poorly known. While π production cross sections can be estimated with some degree of confidence based on experimental data [13], no data at all do exist on η, ω and ρ production. These multiplicities have to be taken either from transport or from statistical thermal models.

2.1 Hadron acceptance

In order to study the response of the HADES spectrometer, first, hadron events generated with the UrQMD transport code [14] were used to determine their acceptance. For simplicity, at this stage of the simulations, we used geometric acceptance matrices instead of propagating the tracks throughout the HADES detection system in GEANT. These matrices were calculated for hadrons as a function of momentum, polar and azimuthal angle, via propagating the particles from a white source through the HADES detector implemented in the HGeant simulation package. Figures 3 and 4 show the simulated acceptances for pions and protons (transverse momentum p_t vs. rapidity representation) in the reaction C+C at 2.0 AGeV and 8.0 AGeV, respectively. Note that HADES was originally designed to study symmetric systems at bombarding energies close to 2 AGeV, where the acceptance of light particles is symmetric around midrapidity.

In these figures the upper frames show the distribution of particles ($\pi^{\pm}$, p) emitted to the full solid angle, whereas the lower frames show the correspond-

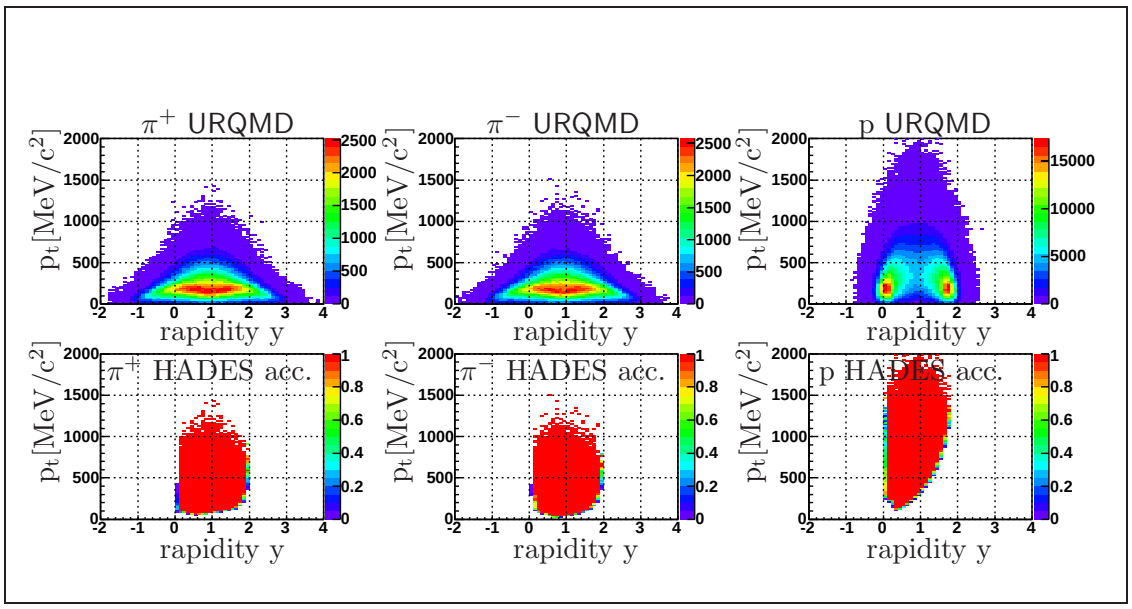

Fig. 3. Distribution of π^+ (left), π^- (middle) and p (right) for C+C at 2.0 AGeV in a (p_t vs rapidity) plot. Upper row: full π phase space. Lower row: within HADES acceptance.

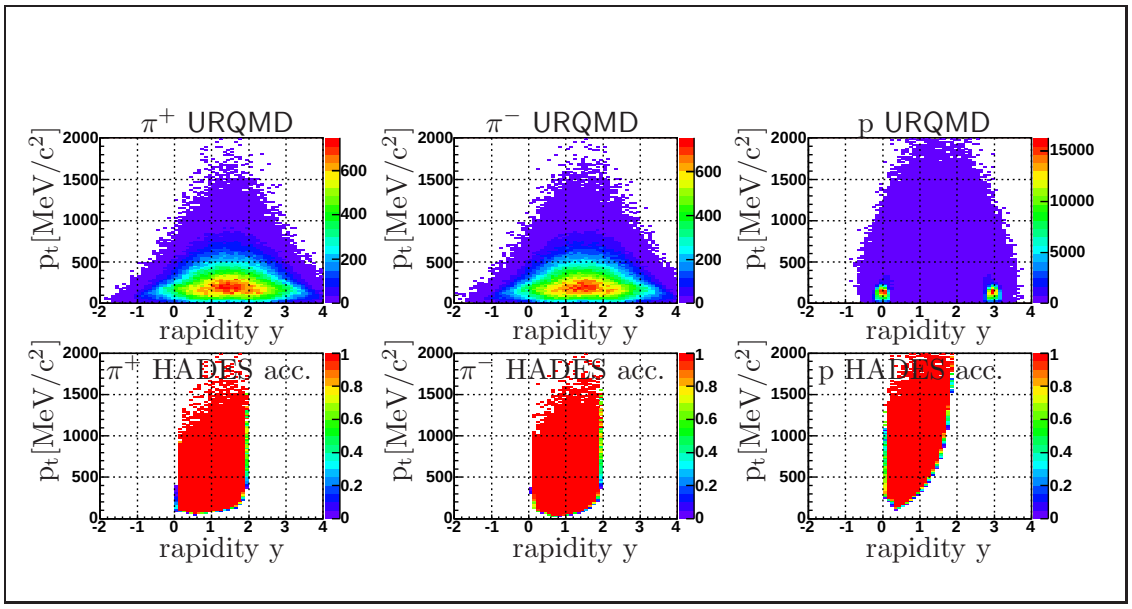

Fig. 4. As Fig.3 but at 8.0 AGeV.

ing acceptance (defined as a ratio of accepted to emitted particles). The region of full azimuthal acceptance, i.e. the part not blocked by the magnet coils (amounting to 83 % of 2 π), is used to normalize the acceptance in the p_t vs. y space. The ratios of accepted particles to those emitted to full solid angle is also listed in Table 1.

particle	2 AGeV	8 AGeV
	Acc.	Acc.
π^+	0.63	0.50
π^-	0.64	0.52
p	0.40	0.15

Table 1
Acceptance of the most abundant hadrons emitted from $^{12}C+^{12}C$ collisions at 2 and 8 AGeV

2.2 Dilepton acceptance

The HADES acceptance for dileptons was studied in a similar way, namely by filtering simulated lepton pairs with geometrical single-lepton acceptance matrices. As an example, of a dilepton source of our interest, we generated pairs from the direct electron-positron decay of the ω meson using the Monte-Carlo generator PLUTO. For the ω meson source, we used a thermal model for the expanding fireball, with inverse slope parameters 89 MeV at 2 AGeV and 105 MeV at 8 AGeV based on UrQMD model predictions and a comparison with experimental data. Individual leptons were propagated through the HADES acceptance filter in the way described above for hadrons, and finally those pairs with laboratory opening angles larger than 9 degrees were retained.

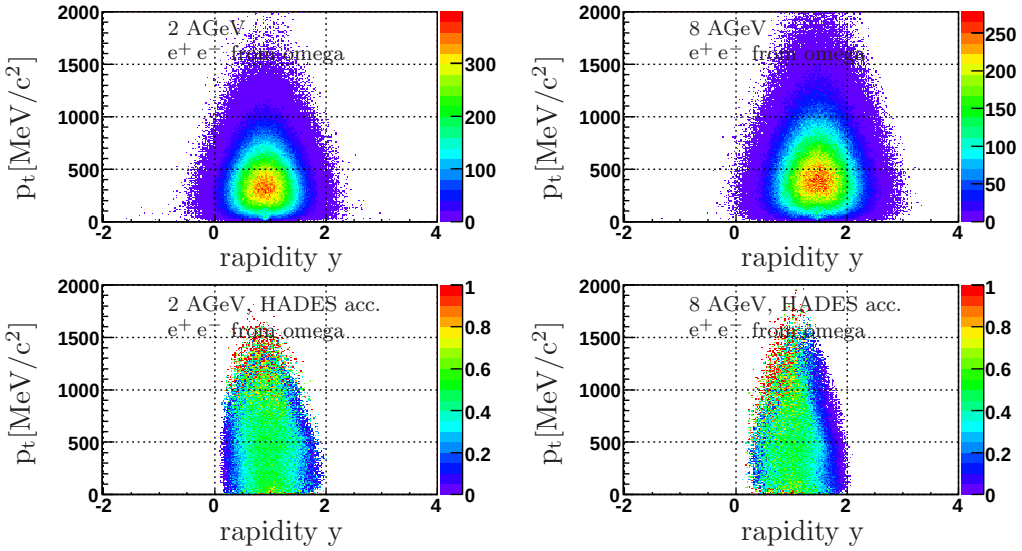

Fig. 5. Top: transverse-momentum vs. rapidity distribution of dielectrons from the direct decay of ω mesons emitted from a fireball at 2 AGeV (left) and 8 AGeV (right). Figures in the lower row show the acceptance in the HADES spectrometer.

In case of 2 AGeV, the overall acceptance for electron pairs is 33 %, while at 8 AGeV it is 21 %. This means that there is only a moderate decrease of the overall acceptance with increasing bombarding energy, due essentially to the stronger kinematic focusing at 8 AGeV. From the distributions shown in Fig. 5 it also follows that the acceptance of HADES with its present geometrical configuration still covers the mid-rapidity region at 8 AGeV. Taking into account the much larger yields of vector mesons expected at the higher energy (see Fig. 2) we can expect significantly higher pair rates in the corresponding region of invariant mass for 8 AGeV, as compared to 2 AGeV, compensating by far the slight decrease in acceptance.

2.3 Rate capability and occupancy of the detector

Hadron multiplicities are expected to increase in the forward part of the spectrometer with increasing beam energy due to the Lorentz boost as well as the enhanced creation of secondary particles in material situated close to the beam axis. In order to achieve decent track reconstruction efficiency, the double-hit probability has to be kept below 20%. These conditions, critical for heavy beams, will be fulfilled after replacing (in 2008) the existing inner TOF system with newly developed fast RPC chambers (see Fig. 6 and section 3.2 on RPC), thereby increasing greatly the granularity and thus the rate capability of the HADES TOF system.

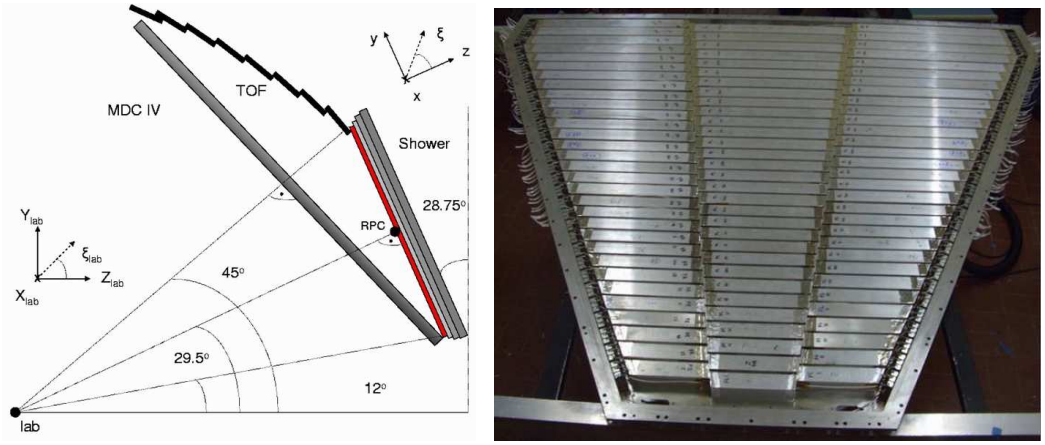

Fig. 6. Left: Geometry of the RPC system. Right: Photography of the timing resistive plate chamber (tRPC) being build for the planned high resolution HADES Time-Of-Flight wall, see section 3.2 for details.

We have carried out simulations of central Au+Au collisions at 1.5 and 8 AGeV with the aim to determine the expected rates and hit densities in the forward polar-angle range. As the particle source we used the UrQMD transport code and the HGeant package for a realistic detector modelling. The

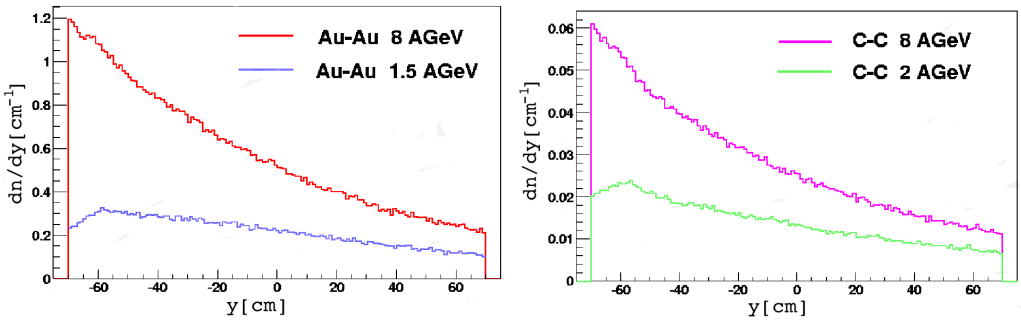

Fig. 7. Simulated hit occupancy on the RPC chambers as a function of y position for central Au-Au (b<4 fm) and C-C (b<3 fm) collisions for 2 different beam energies, corresponding to the present SIS18 (maximum energy) and the future FAIR facility, respectively [15]. Results have being obtained with URQMD for event generation and HGeant for transport.

present HADES detector geometry was implemented. As shown in Fig. 7, by changing the colliding system from C+C at 2 AGeV to Au+Au at 1.5 AGeV (maximum SIS18 energies) the rates increase significantly, namely by a factor of 14, whereas the increase in beam energy causes a rise of the maximum occupancy by only a factor 3.4 (Au+Au at 1.5 AGeV in comparison with Au+Au at 8.0 AGeV). The simulation results show that we can expect about 20% double hit probability for Au+Au at 1.5 AGeV which will be already a challenge mainly for the tracking system in the forward part of the spectrometer. In terms of the hit occupancy the Au+Au at 1.5 AGeV can be roughly compared to the Ni+Ni system at 8 AGeV and thus this system is considered as the heaviest system handled by HADES at SIS100 (see subsection 4.1).

2.4 Dielectron cocktail

Finally, we simulated the full "dielectron cocktail", generating all dilepton sources simultaneously using the PLUTO generator with realistic models of resonance production, as well as hadronic and electromagnetic decays. The simulation was done for the C+C and Au+Au systems at 8 AGeV, and for the sake of a comparison, also for C+C at 2 AGeV and Au+Au at 1 AGeV. The generated events were filtered through the HADES geometrical acceptance filter. Finally, lepton momenta were smeared appropriately to take into account the detector resolution.
The analysis of the events was carried out as follows:

- For all possible combinations of electrons and positrons an opening-angle cut $\theta_{ee} > 9°$ was applied. (If a pair did not pass this condition, both leptons were excluded from the sample.)
- If the remaining pairs belonged to the same source particle, they were

counted as a signal.

- If not, they were put to the combinatorial background.

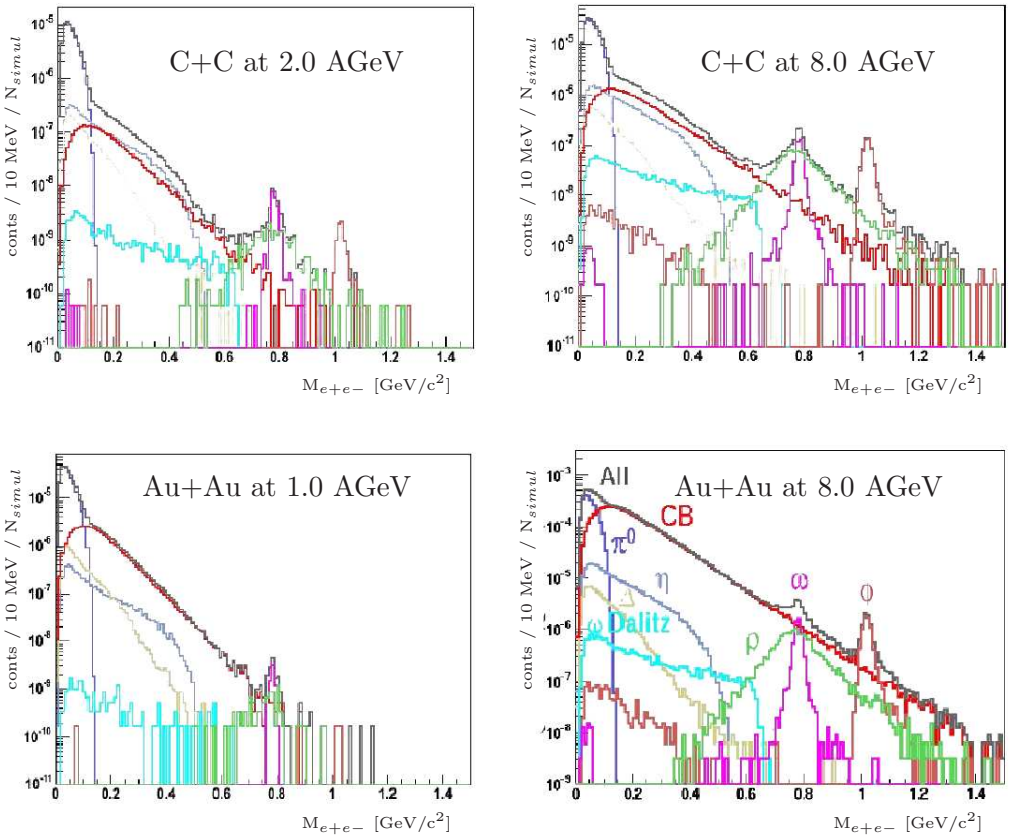

Fig. 8. Top: Simulated invariant-mass distribution of dielectron pairs per collision detected in HADES from C+C colisions at 2 AGeV (left frame) and at 8 AGeV (right frame). Bottom: Same for Au+Au at 1 AGeV (left panel) and at 8 AGeV (right panel). Fully simulated cocktail (black line) and combinatorial background (red line), as well as various cocktail components are shown.

Resulting invariant-mass spectra for C+C collisions with $b = 0 - 2fm$ (17.5 participants in average) and for the Au+Au collisions with $b = 0 - 8fm$ (228 participants in average) are shown in Fig. 8. The huge gain in the expected yield around the omega pole at higher energies is apparent, the yield from direct ω and ϕ decays increases by factors of 29 and 73, respectively, when increasing the beam energy from 2 AGeV to 8 AGeV. With an equivalent of 10^9 triggered events stored on disc during one typical two-week HADES run, we expect to reconstruct more than 25000 pairs from ω and ϕ decays.

2.5 Reaction-plane reconstruction

Future HADES experiments at FAIR will further profit from a Forward Hodoscope (FH) consisting of 288 plastic scintillator cells, which has been added

to the HADES setup in 2007. The FH was already used in 2007 to detect spectator protons in the break-up of projectile deuterons with an energy of 1.25 AGeV.

In future heavy-ion experiments this device will largely improve the event-characterization capabilities of the experiment, namely its ability to measure event-wise the impact parameter and reaction plane. The corresponding feasibility study was carried out using again events for Au + Au generated with UrQMD in a similar way as described above. Those events were divided into three bins in centrality:

(1) central: b $<$ 5 fm
(2) semi-central: 5 fm $<$ b $<$ 10 fm
(3) peripheral: 10 fm $<$ b.

In the simulation, the FH, consisting of 140 small cells (4x4 cm^2), 64 middle cells (8x8 cm^2) and 84 big cells (16x16 cm^2), was positioned seven meters downstream from the target. The occupancy of single cells is shown in Fig. 9 for semi-central Au + Au collisions at 1.0 AGeV compared to those at 8.0 AGeV; it stays below 0.5 in all cases. It should also be noted that UrQMD provides only spectator nucleons and no fragments, i.e. it overestimates the nucleon multiplicity, affecting mostly the inner part with 20 cm radius.

The occupancy increases only about a factor two going from SIS18 to low FAIR energies. The reaction-plane angular resolution σ deduced from proton hits in the FH is about 48 degrees, which has to be compared with the theoretical value of 46 degrees deduced from all protons emitted into the forward hemisphere in Au+Au collisions at 8 AGeV, see Fig. 10. Here the reaction plane was reconstructed from events with more than 8 hits in FH.

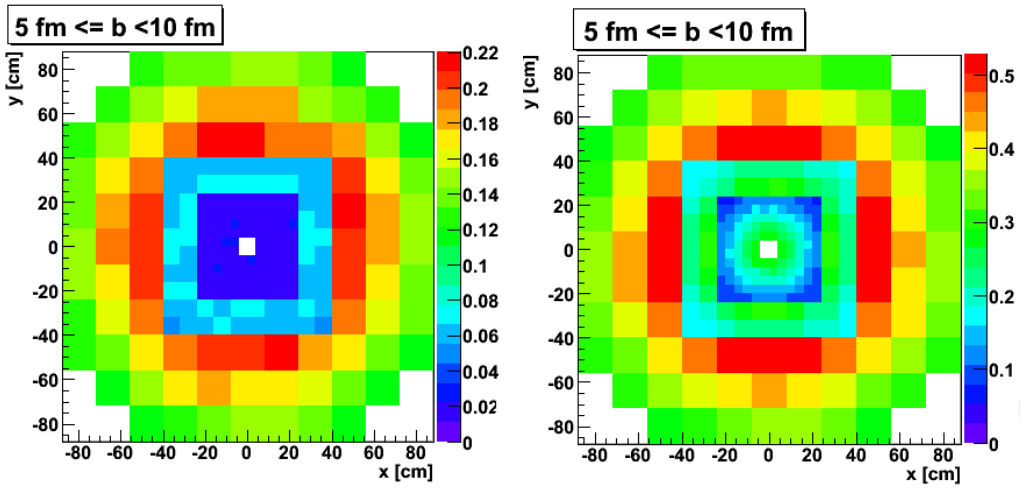

Fig. 9. Occupancy of single cells for semi-central Au + Au collisions at 1 AGeV (left) and 8 AGeV (right).

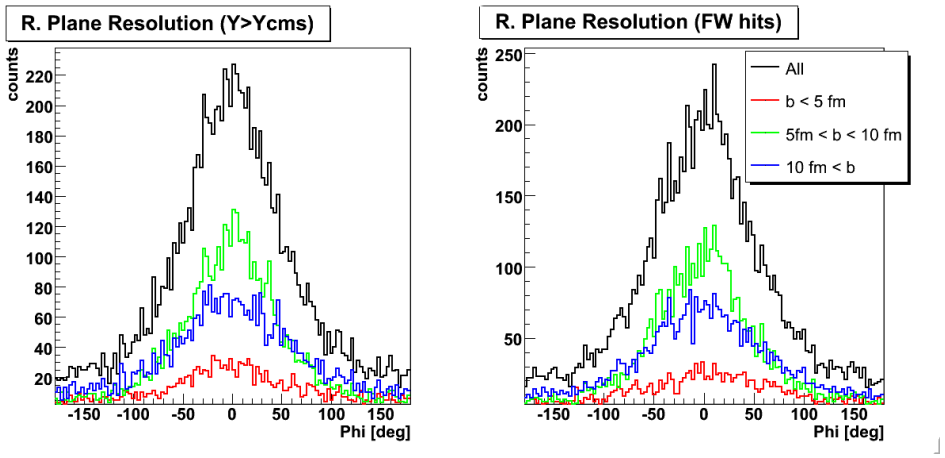

Fig. 10. Reaction plane resolution reconstructed from all protons with y> y_{cms} (σ = 46 deg, average event) (left) and reconstructed from only those protons hitting the FW (σ = 48 deg, average event) (right).

3 The HADES upgrade projects

3.1 Current performance

The HADES spectrometer is a universal device able to investigate a variety of probes in various collision systems. Even though it was designed and optimized with the goal to perform high-accuracy dielectron spectroscopy, it is also suitable for high-resolution hadron spectroscopy, as demonstrated by successful studies of strangeness production, as well as by our programme of spectroscopy in elementary pp and pn reactions. Several experimental runs performed with different systems and at various colliding energies proved the required performance of the device. An extensive description of its performance is presented in [18].
However, due to the low granularity of the inner TOF system (TOFINO), the present setup of the spectrometer can be used for rather light collision systems only (up to Ca+Ca). To equip HADES for experiments with heavy systems at SIS18 and, even more so, for runs at FAIR, a comprehensive upgrade programme has been started which consists of several subprojects described in this section.

3.2 RPC

A new TOF Wall based on the timing resistive plate chambers (tRPC) technology [12] is being built to equip the low polar-angle region of the spectrometer ($\theta < 45°$) with the granularity and time resolution needed to cope with high-

multiplicity events.
The tRPC technology offers very good time resolution, better than 100 ps (σ) and high efficiency (close to 100%) at reasonable cost. Also, a tRPC-based detector can be made very compact, efficiently using the scarce space available between the outer MDC planes and the Pre-Shower chambers.
The newly designed RPC TOF detector will replace the low-granularity inner TOF system, the so-called TOFINO. With 1200 individually shielded 4-gap tRPC detectors, the RPC TOF wall will allow the spectrometer to handle multiplicities of up to 200 charged particles per event. It will furthermore be integrated into the first-level multiplicity trigger and, due to its superior time resolution, it will improve the electron and hadron identification in synergy with the existing Pre-Shower detector [16].
A maximally overlapping 2-layer design is used for full geometrical coverage. It also includes a degree of redundancy, which allows excellent timing-tail suppression for optimum TOF identification of heavy rare particles, like e.g. charged kaons.

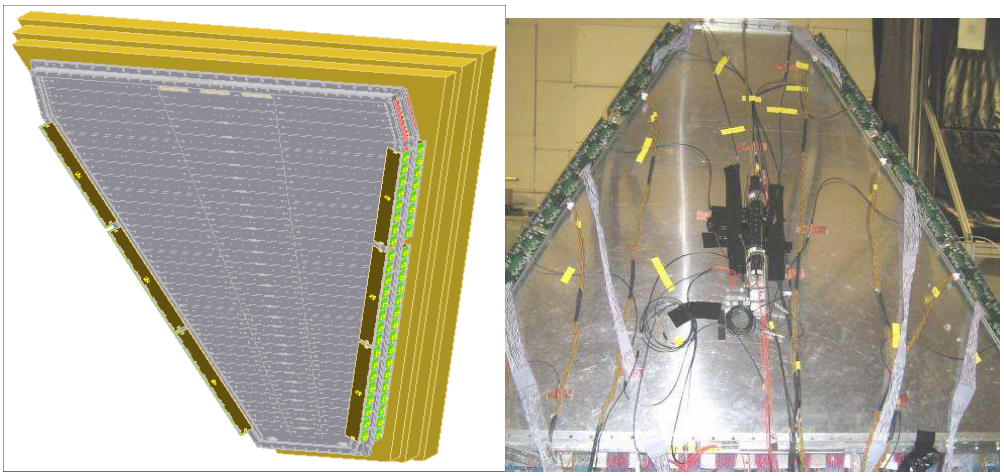

Fig. 11. Left: Geometry of the new tRPC TOF wall. There are 200 individually shielded detectors in each of the 6 sectors, organized in two maximally overlapping layers and 3 columns. The redundant time measurement will provide excellent TOF information for identification of rare heavy particles. Right: Prototype mounted in HADES during a full sector test.

The RPC front-end electronics will use compact, wide-band, low-noise amplifying and digitizing chips filling the tight room formed by the shadows of the superconducting coils. Digital LVDS output signals will codify both the time and charge information and will be read out by the TRB [25] system: a modern and powerful DAQ concept that will be extended to most of the HADES detectors.
A full sector test was performed in November 2007 with very positive results on time resolution (85 ps (σ) average resolution), efficiency (over 95%),

crosstalk (less than 1%), geometric coverage and mechanical, electromagnetic and software integration into the HADES setup.

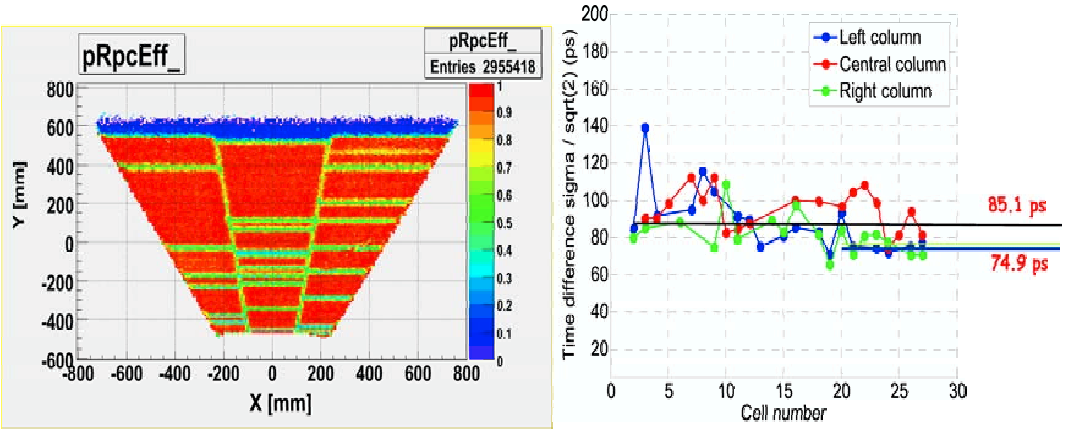

Fig. 12. Full-system test results. Left: Efficiency map and geometric coverage. Gaps correspond to defective electronics channels and the location of the features is convoluted with the MDC resolution in low-res analysis mode. Right: Time resolution measured between pairs of overlapping RPC cells: the system average is 85 ps, while in a restricted region the average is 75 ps.

3.3 Rebuild of MDC Plane I

In the Forschungszentrum Dresden-Rossendorf (FZD) new multiwire drift chambers (MDC) for replacement of the six innermost chambers of HADES (MDC1) has been constructed. The aim of these new detectors is to guarantee high spatial track resolution of about 0.1 mm for charged particles with a counting efficiency close to 100 % in heavy-ion collisions at beam energy of up to 8 AGeV. To measure rare reactions, the rate capability of the MDC1 must be sufficient for the envisaged high luminosities at FAIR. The new chambers will be installed in 2009. The workshop at FZD is producing seven completely equipped chambers.

The design of the new MDC1 differs conceptually from that of the former detectors, whereas the shape of the frames, the keep-in volume of the detector, as well as the drift-cell geometry (5x5 mm^2) must be conserved. The former MDC1 chambers were composed of six power frame layers. Each power frame consists of a 2.5 mm thick Stesalit frame and a 2.5 mm thick stainless steel frame. The new MDC1 will be assembled from 13 individual self-supporting glass-fiber epoxy (Durostone) frames. Because the elasticity modulus of Durostone sheets is one order of magnitude lower than that of steel, the expected larger deformation of the frames has been calculated with a finite-element method to make a precise forecast of the position of the calibration holes such

as to merge an anode and a cathode layer each, thus compensating their respective deformations. This functional principle has been demonstrated in a prototype test.
The gas distribution system comprises four inlets and two outlets per chamber. To guarantee a homogeneous gas distribution in the whole chamber volume, the He/isobutane mixture flows through all 13 anode/cathode layers. To improve the gas tightness, the number of stiffening bolts has been doubled with respect to the former design.

In the new MDC1, CuBe (75 μm) wires replace the former Al (80 μm) wires. The advantage of CuBe wires is the better long-term stability of the wire tension and ohmic contacts. A disadvantage, however, is their lower elasticity, demanding higher mechanical precision during chamber manufacturing and assembly. The anode planes are made of gold-coated tungsten wires of 20 μm diameter. Impedance-controlled stiff-flexible PCBs connect the signal wires to the front-end electronics. The impedance adaptation is chosen to reduce noise and cross talk. Electronic noise will be reduced further by implementation of 13 individual HF filters into the high-voltage power-supply lines. These filters will be mounted directly behind the HV PCB.

3.4 RICH simulations for higher beam energies

Experiments at higher beam energies are characterized by an increase of particle multiplicities per event and reaction kinematics with a more pronounced emission of faster particles to forward polar angles. With the currently used radiator geometry, the RICH performance and its electron/hadron discrimination capability are expected to suffer from three effects at FAIR energies:

(1) Photon background from pion-induced Cherenkov light due to an increase of the average particle momenta.
(2) Lower average detection efficiency for $e^{\pm}$ due to the more forward-oriented emission, i.e to polar angles with shorter radiator lengths.
(3) Larger hit background in the photon detector originating from γ and charged reaction products due to increased particle multiplicities per event, in particular for heavy collision systems.

Since the RICH is used as an online trigger device for events with $e^{\pm}$ content, the advent of these effects has considerable impact on the overall performance of the HADES detector.
A rearrangement of the mechanically coupled RICH/target system accompanied by a moderate (by a few cm) upstream shift with respect to the magnetic field and the innermost drift chambers may help to optimize the RICH exposure. The prohibitive cost of a new mirror and photon detector rule out, however, a complete RICH redesign. Therefore, we have studied three scenar-

ios, in which only the radiator is modified, namely by:

- Use of different radiator gases
- Extension of the radiator length
- Upstream shift of the photon detector

Table 2 lists possible gases and mixtures which match the VUV transmission cutoff of the CaF_2 entrance window and provide a reasonable number of primary photons per ring for the given range of radiator lengths.

Radiator gas	λ_{cutoff} [nm]	n - 1 [10^{-3}]	γ_{thr}	$p_{thr}^{\pi^\pm}$ [GeV/c]	$N_{>thr}/N_{4\pi}$ [10^{-3}] 8.0 AGeV	$N_{>thr}/N_{4\pi}$ [10^{-3}] 15 AGeV
C_4F_{10}	145 nm	1.410	18	2.4	8.9	47.4
C_4F_{10}/CH_4	147 nm	1.030	22	2.97	2.0	18.8
C_2F_6	136 nm	0.793	25	3.3	0.91	10.8
CH_4	147 nm	0.510	31	4.2	0.09	2.5

Table 2
Optical properties, pion momentum thresholds and fractions of pions that emit Cherenkov light for various radiator gases.

We have systematically investigated all combinations using the standard HADES software packages (PLUTO++, HGeant and HYDRA) for event generation, particle transport, and detector signal analysis, respectively, with experimentally verified detector parameters and unchanged ring-search algorithms. The simulations were performed for the decay channels $\omega \rightarrow e^+e^-$ and $\omega \rightarrow \pi^+\pi^-\pi^0$ of omega mesons emitted from a thermal source with temperatures of 72 MeV, 85 MeV, 108 MeV, and 125 MeV and, for a more realistic scenario, with UrQMD-based C+C collisions at E_{kin} = 8.0 AGeV. The results of this detailed study are compiled in [21].

Figure 13 shows that for a $C_4F_{10}/CH_4(1:1)$ or C_2F_6 radiator the fraction of pions generating Cherenkov photons is reasonably small up to E_{kin} = 8.0 AGeV. For heavier charged hadrons (kaons, protons etc.) the detector stays blind. Since for pions the ring radii ($\overline{R} \simeq 8 \pm 3mm$) and number of primary photons per ring ($\overline{N_{phot}} \simeq 6 \pm 3$) are considerably smaller than for electrons, they can be separated and suppressed in the data analysis and even already in the second-level trigger. Experiments at energies $E_{kin} \simeq 15.0$ AGeV with a pure CH_4 radiator, however, do not seem feasible, since the number of detectable photons per ring is by far too low.
The optimum radiator geometry is based on an extension of the radiator ves-

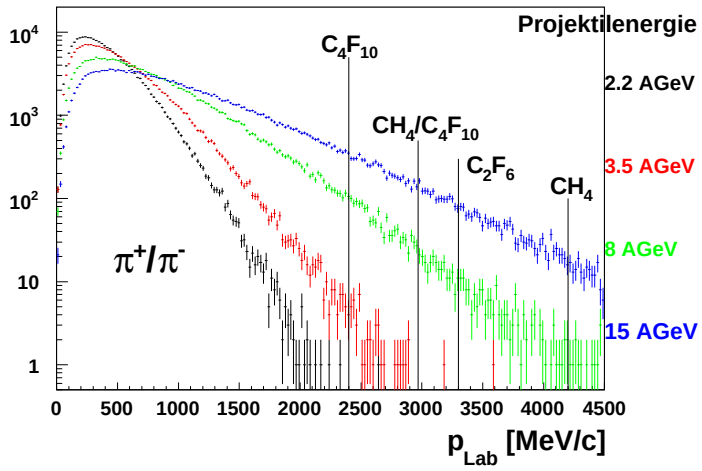

Fig. 13. Pion momentum distributions for thermal ω decays at various projectile energies. The Cherenkov thresholds are shown for four radiator gases.

sel by 150 mm and a global upstream shift of the RICH of 200 mm. Inside the vessel, the photon detector is shifted by 50 mm. The resulting poorer optical quality of the, somewhat out-of-focus, ring images is over-compensated at forward polar angles by an increase in the number of firing pads per ring. Hence, the single $e^{\pm}$ detection efficiencies in the ρ/ω mass region increase (see Fig. 14). These results lead us to the conclusion that the proposed RICH mod-

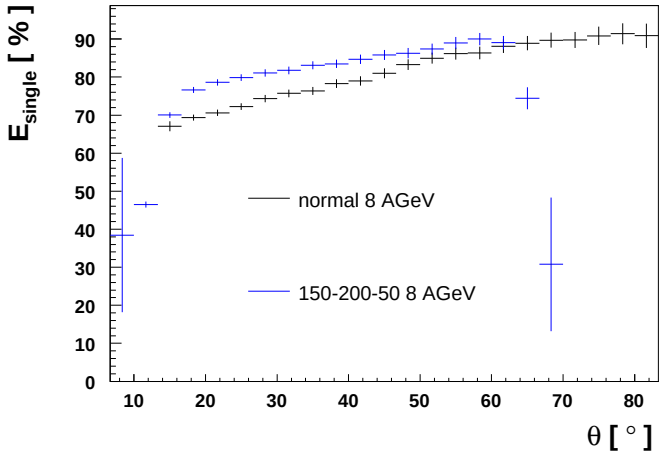

Fig. 14. Expected single $e^{\pm}$ detection efficiencies for $\rho \rightarrow e^+e^-$ decays in C+C collisions at $E_{kin} = 8.0$ AGeV for the standard and a modified geometry (see text). The events were generated with the UrQMD trasnport code.

ification is a valuable choice. Moreover, it would already be beneficial for the HADES physics program at low energies, as it will be pursued in the coming five years. An additional global upstream shift of the RICH/target system would readjust the geometrical spectrometer acceptance to mid-rapities, but is not mandatory.

In any case, the proposed modification would provide the opportunity to reduce the material budget surrounding the target area which in turn would reduce the conversion background, while leaving space for additional solid-state detectors (diamond, silicon strip, etc.) with their readout cables. This would open new and promising possibilities for fast trigger devices and high-multiplicity tracking support.

3.5 DAQ concept

As mentioned earlier in this document, HADES is planning experiments with larger collision systems at higher beam energies and, generally, aiming for higher statistics. These objectives result in number of experimental challenges, such as very high interaction rates and hit-densities in the detector. Therefore, the requirements on the trigger, the data acquisition and the online data processing will be greatly increased, making an upgrade of the DAQ system necessary.

The present multi-level trigger system used by HADES at the SIS18 heavy-ion synchrotron consists of a level-1 (LVL1) trigger, based on the charged-particle hit multiplicity in an array of scintillator detectors (the TOF), and a level-2 (LVL2) trigger system, which selects events by searching for lepton pairs. A "Central Trigger System" (CTS) generates the trigger signals. The CTS consists of a "Central Trigger Unit" (CTU) and a "Matching Unit" (MU). The trigger number and the physics source of the triggers are contained in the digital trigger information generated by the CTU; this information is transmitted to all detector subsystems. The data from the individual detector systems are buffered in a LVL1 pipe where it is waiting for the decision of the LVL2 trigger system. In case of a positive LVL2 trigger decision (based on online pattern recognition in the detector subsystems), the data is stored in a LVL2 pipe and sent to event builder. The data reduction factor achieved by the LVL2 trigger ranges from 1:3 to 1:9, depending on the multiplicity in the detectors. Typical trigger rates for the reaction ^{40}Ar+^{39}K^{35}Cl are 7 kHz and 1 to 2 kHz for LVL1 and LVL2, respectively.

The addition of the newly developed resistive-plate chambers (RPC) [19,20], the limited LVL1 rate, insufficient data reduction of the LVL2 trigger system, as well as the large data rates expected in Au+Au collisions at SIS18 and FAIR, requires an upgrade of the HADES trigger and readout system. The aim is to reach at minumum a LVL1 accepted event rate of 20 kHz, even when running with the highest expected multiplicities in the detectors.

A key point of the DAQ upgrade is the development of the "Trigger and Readout Board" (TRB). This multi-purpose electronics device with on-board DAQ

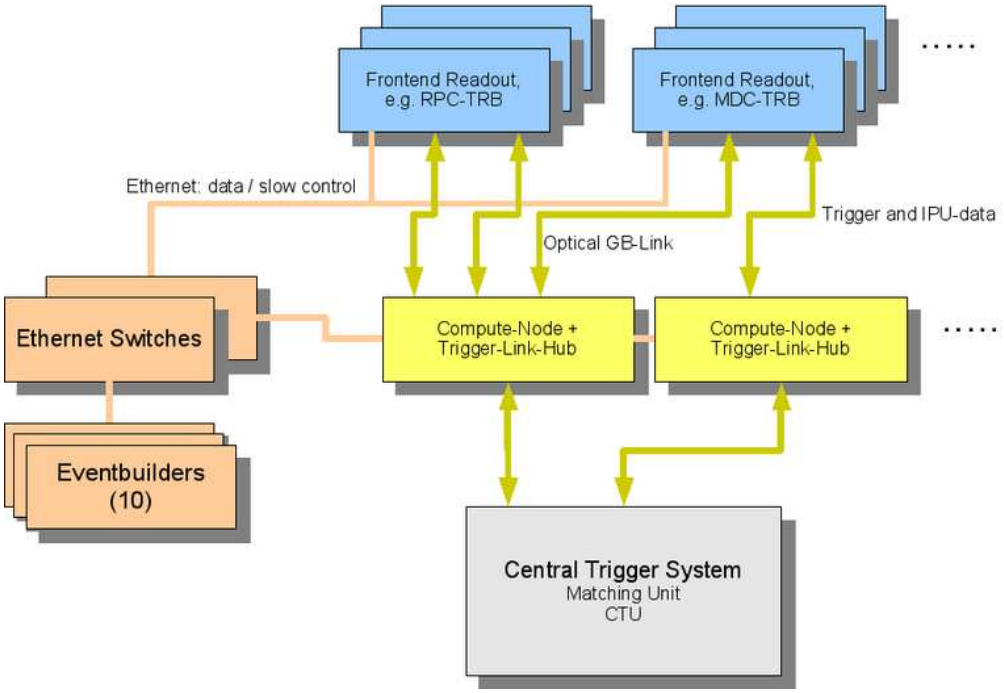

Fig. 15. Architecture of the new DAQ/Trigger system.

functionality was originally designed for the new RPC detector. As the first version of the TRB (TRBv1 [22]) was successfully tested during the HADES data taking periods it was decided to extend its design to the new standard readout module TRBv2 [23] for all HADES subdetectors. The architecture of the upgraded DAQ system is shown in Fig. 15. The readout of the detector-specific FEE, LVL1 pipes, interfaces for special connectors/electrical standards and additional computing resources are provided by detector-dependent add-on boards which can be mounted on the TRBv2 using a very high data rate digital interface connectors. The present trigger distribution bus-system will be replaced by a tree-like trigger distribution via optical TRB-Hubs with only point to point links, realized with 2 Gbit/s optical links, which results in 200 MB/s raw data rate. These high-speed optical links can also be used for the transport of LVL2 trigger data to the planned LVL2 trigger computing nodes. Each computing node will consist of an array of FPGAs with a set of IO capabilities.

For easy monitoring and operation of the large number of modules needed, the TrbNet, a new hardware-independent network protocol is developed. It allows the simultaneous (interleaved) distribution of trigger information, which has to be done with a low latency (below $1\mu s$), and the transportation of large amounts of data using only one data link. Different logical channels provide priority levels, while buffers on each connection guarantee protection from data loss. The protocol also offers a slow-control channel to dynamically switch on and off parts of detectors or to read out status and error information. New devices can be included into the network as easily as merely connecting them

to a hub (plug and play). Every network node can be configured with a wide range of parameters to adopt to existing or new hardware and their specific requirements.

The considerable effort is being devoted to the development of the LVL2 trigger algorithm for very high multiplicity events. The largest computing challenge is posed by MDC detector, which requires real-time recognition of complex patterns. It might be hard to find unambiguous patterns in the data to achieve sufficient data reduction in heavy-ion collisions. Therefore the DAQ system should be able to accumulate all the possible data rates in the absence of the LVL2 trigger. In these experiments (e.g. Au+Au collisions) the highest expected total data rate at 20 kHz LVL1 trigger rate is estimated to be 300 MB/s. In a parallel event-building process a number of input data paths from the TRBs are connected to a number of output data paths to the event builders and all the data paths can be active simultaneously to maintain the aggregate band width. Ten event builders will decrease the highest achievable data rate of 300 MB/s down to 30 MB/s and the event rate of 20 kHz down to 2 kHz per event builder. At this reduced data load, the currently existing event builders show stable operation with 90 data sources. More details about the HADES-DAQ upgrade can be obtained from [25].

3.6 Calorimeter for HADES

Dielectron results obtained at SPS and RHIC demonstrate a large pair excess in the intermediate ($0.14 < M < 0.6 GeV/c^2$) mass region. A precise determination of this excess depends on precise knowledge of the hadronic cocktail, which for 2-40 AGeV is dominated in this mass region by the η Dalitz decay. Furthermore, a convenient normalization of the dielectron spectra is naturally given by the π^0 yield. For the SIS18 energy range, production of neutral mesons has been studied extensively by the TAPS collaboration via photon calorimetry. However, for the 2-40 AGeV range no data at all do presently exist, with the consequence that any interpretation of future dielectron data would have to depend solely on theoretical models, e.g. transport calculations or appropriate hydrodynamical models. In order to remedy this situation we propose to measure the respective π^0 and η meson yields together with the dielectron data. This can be achieved by replacing the HADES Pre-Shower detector, located at forward angles ($18^\circ < \theta < 45^\circ$), with an electromagnetic calorimeter of some sort, preferentially in such a way as to stay compatible with the planned CBM calorimeter. An additional advantage of such a device would be the better electron/pion suppression that it offers at large momenta (p>400 MeV/c) as compared to the present situation. Note that at lower momenta the electron/hadron identification is provided by the RICH, RPC and TOF detectors.

The total area required for a HADES calorimeter amounts to about $8\,\mathrm{m}^2$ and could be realized in the "shashlik" sampling scintillator-lead technique, also proposed for CBM. The energy resolution which can be achieved using the shashlik technique varies between $3\%/\sqrt{E}$ to $6\%/\sqrt{E}$, depending on the so-called volume ratio, i.e. the ratio of scintillator to converter material. According to simulations, the best resolution is achieved for the configuration of 300 layers of scintillator/lead with 1 mm/0.5 mm. Since particle rates expected for HADES at FAIR will be much lower than for CBM in general, the CBM larger-size modules of 6x6 cm^2 (foreseen for the middle part of the CBM calorimeter) would be sufficient. In order to cover the Pre-Shower area, 1440 modules, 240 per sector, are needed. These modules will be arranged in rows with varying number of columns such that they fill trapezoidal volumes.
Another option, which is currently under investigation, is to recuperate a lead-glass calorimeter from the former OPAL experiment at LEP and adapt it to HADES. The existing OPAL modules are larger (9.4x9.4 cm^2) and their use would hence result in smaller granularity (840 modules in total). The energy resolution of this solution is comparable to the one of shashlik modules, amounting to 6% at 1 GeV.

The detector acceptance and resolution have been studied using Monte Carlo. It was assumed that the calorimeter is positioned at a distance of 2.4 m from the target (the nominal position of the present Pre-Shower detector) and the size of a single module used for the simulation was 4x4 cm^2 thus the spatial resolution (SR) of a single module is: σ_θ, σ_ϕ of the order of 0.8 mrad.

Figure 16 presents the geometrical acceptance of the proposed HADES calorimeter for eta meson decays ($\eta \rightarrow \gamma\gamma$) as a function of transverse momentum and rapidity.

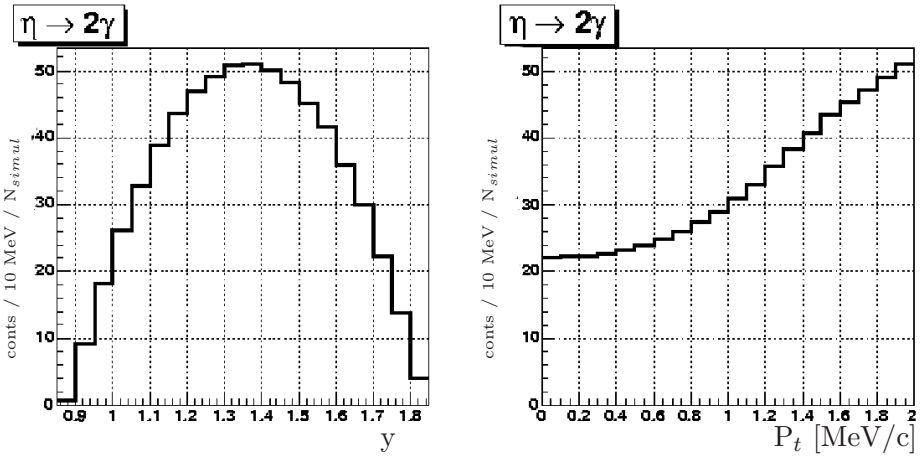

Fig. 16. Geometrical acceptance of calorimeter for eta mesons as a function of rapidity (left) and transverse momentum (right). The calorimeter was located 2.4 m from the target, covering $18^\circ < \theta < 45^\circ$.

Figure 17 shows the reconstructed two-photon invariant-mass distributions for the eta signal (red) and combinatorial background (blue), assuming the granularity of the shashlik calorimeter described above. Particle distributions have been generated with the UrQMD transport model for C+C (left) and Ni+Ni (right) collisions at 8 AGeV with the following π^0 (η) multiplicities: 2.6 (0.21) for C+C and 15 (1) for Ni+Ni. An energy resolution of $3\%/\sqrt{E}$ and 0.8 mrad angular resolution, given by the size of modules, have been assumed.

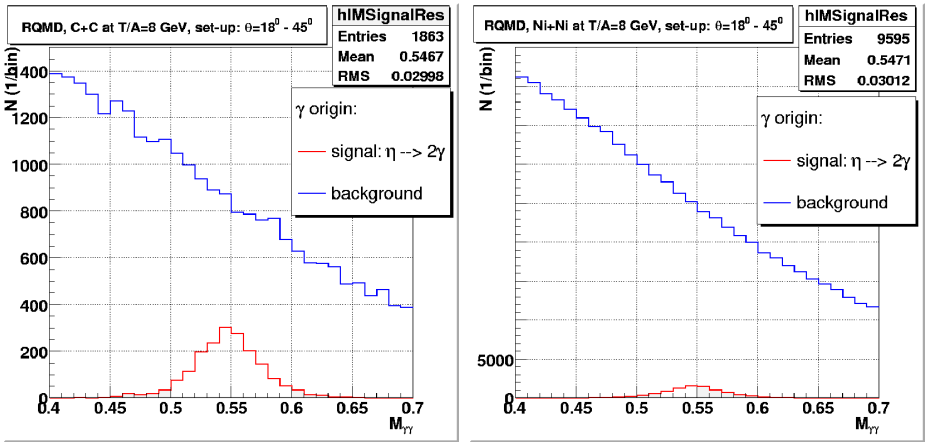

Fig. 17. Two-photon invariant-mass distributions in C+C (left) and Ni+Ni (right) collisions at 8 AGeV, reconstructed for the eta signal (red) and the combinatorial background (blue).

Table 3 presents a compilation of signal-to-background ratio and statistical significance, defined as $\sqrt{(signal)}/B$, obtained for various systems, beam energies and resolutions. It was found that a cut on the momenta of the reconstructed photons improves the signal-to-background ratio. In the results presented in the table a photon momentum cut of 300 MeV/c has been applied.

	Signal/Background (S/B) ratio [%] / **Significance** $\sqrt{(signal)}/B$		
System	perfect ER SR: σ_θ, σ_ϕ 0.8mrad	ER: $3\%/\sqrt{E}$ SR: σ_θ, σ_ϕ 0.8mrad	ER: $6\%/\sqrt{E}$ SR: σ_θ, σ_ϕ 0.8mrad
C+C 2 AGeV	201/40	43/26	22/20
C+C 8 AGeV	53/25	16/15	10/12
Ni+Ni 8 AGeV	10/29	3/16	2/12

Table 3
Signal-to-background ratio (in %) and significance of the reconstructed η signal for various collision systems assuming three different values for energy resolution (ER) and spatial resolution (SR) of σ_θ, σ_ϕ 0.8mrad.

4 HADES at FAIR

4.1 Beam requirements

As outlined in the *Physics Motivation* chapter, the HADES collaboration aims at performing a systematic study of dilepton production at the planned FAIR facility in the energy region of 2-10 AGeV with, both, proton and HI beams as a continuation of the HADES physics program started in 2002 at SIS18. Dilepton production at these energies is hardly known and only very limited data exists. On the other hand, HADES is foreseen as an experiment ready to take data once the new accelerator facility is operational, as well as during the assembly and commissioning phase of the CBM experiment. As specified in the *FAIR Baseline Technical Report, Table 2.1*, slow extraction from both SIS 100 and SIS 300 is planned, which is essential for our experimental activities at the FAIR accelerators.

Experiment	Energy [AGeV]	intensity [part./sec.]	duration
p+p	8, 10	$5.0{\cdot}10^8/s$	2×2 weeks
C+C	4, 10	$2.0{\cdot}10^7/s$	2×2 weeks
Ca+Ca	4, 10	$6.0{\cdot}10^6/s$	2×2 weeks
Ni+Ni	4, 10	$4.0{\cdot}10^6/s$	2×2 weeks

Table 4
Proposed HADES runs at FAIR.

The proposed timetable of the planned experiments at the FAIR facility takes into account the experience and the knowledge gained with HADES at SIS18. The HADES collaboration intends to perform two experiments per year. In addition, two to three test runs should be scheduled, once the installation of the HADES spectrometer in the CBM cave is completed. The total duration of experimental activities of HADES at FAIR can thus be estimated to be of the order of six to seven years.

Table 4 summarizes the beam intensities and reaction systems planned for the HADES dilepton experiments. Rough estimates of the duration of these runs are also given.

In order to provide optimal experimental conditions for dilepton spectroscopy, the following requirements related to the beam properties have to be fulfilled.

- One of the main contributions to the combinatorial background of the dilepton invariant-mass spectrum comes from the gamma conversion process taking place in the target material. In order to minimize this, HADES has to use small-size segmented targets: a disc shape with a diameter of 2 mm and

total thickness of about 1 mm (should correspond typically to about 1% reaction probability) which imposes severe limits on the size of the beam spot at the HADES focal point, namely to be of the order of or less than 2 mm diameter (enclosing 90 % beam intensity). The acceptable amount of beam particles at a distance greater than 5 mm away from the beam symmetry axis (beam halo) should be kept below 10^{-5} of the full beam intensity. This condition also holds for segmented targets with a total longitudinal extension of up to 50 mm. In the end, data taken with heavy ions will still be dominated by combinatorial background whose subtraction will result in an increase of the overall error by a factor of two or more.

- The next aspect which defines our requirements is the beam hole of 6 cm diameter in the HADES forward wall detector, located about 7 m downstream of the target. As a consequence, a rather small beam divergence is needed at the HADES focal point. Based on the considerations presented above, the required beam emittance at the target point can be estimated to be in the order of 5×10^{-6} $\pi \times m \times rad$ for Ca + Ca @ 5 AGeV. It could be 30% larger at the smallest energies (2 AGeV) and should be about 30% smaller at the highest energies 8 A GeV.
- Finally, for HADES it is important to keep the beam intensity fluctuations below 50%, down to the 50 microsecond time scale, in order to provide stable operation conditions for the detectors, mainly the wire chambers, and to allow for an effective use of the beam (without large dead-time fluctuations).

4.2 Cave design

The amount of space needed for the HADES spectrometer in the CBM cave is optimized based on the experience gained during work in the present HADES cave. The size of the existing cave and the location of the spectrometer in the cave (see Fig.18) is the minimum needed. The HADES main frame is located in the middle of the cave and the distance to the wall is about 2 m and 3 m, on the left and right side, respectively. Part of this space (about 1 m) is used for electronics and HV supply racks, whereas the rest is kept free to allow access to the spectrometer from the side. At the rear of the cave, dedicated free space is provided for temporary storage during installation, servicing and preparation of the subsystems before installation into the main frame. The minimal amount of space in front of the main frame should be 4 m. It is needed for the operation of the spectrometer and can not be reduced further. Thus, the dimensions quoted here define the minimal space required for the spectrometer at FAIR and should be used during the design of the new cave.

A drawing of the geometry of the new HADES/CBM cave, showing the placement of the HADES spectrometer and the proposed CBM detector within the hall is given in Fig. 19 and Fig. 20. Although the overall size of the new cave will be much larger than the one of the present HADES cave, the available

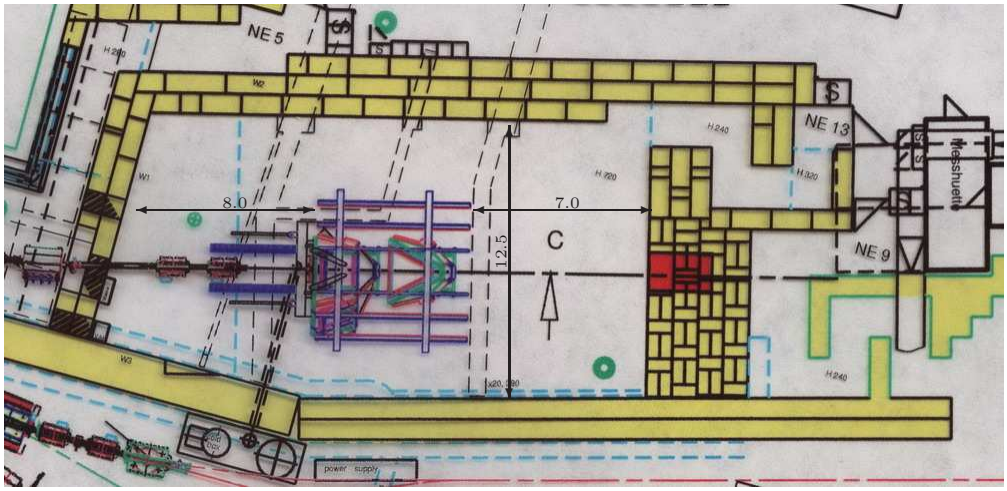

Fig. 18. Layout of the present HADES cave at SIS18, showing the placement of the spectrometer.

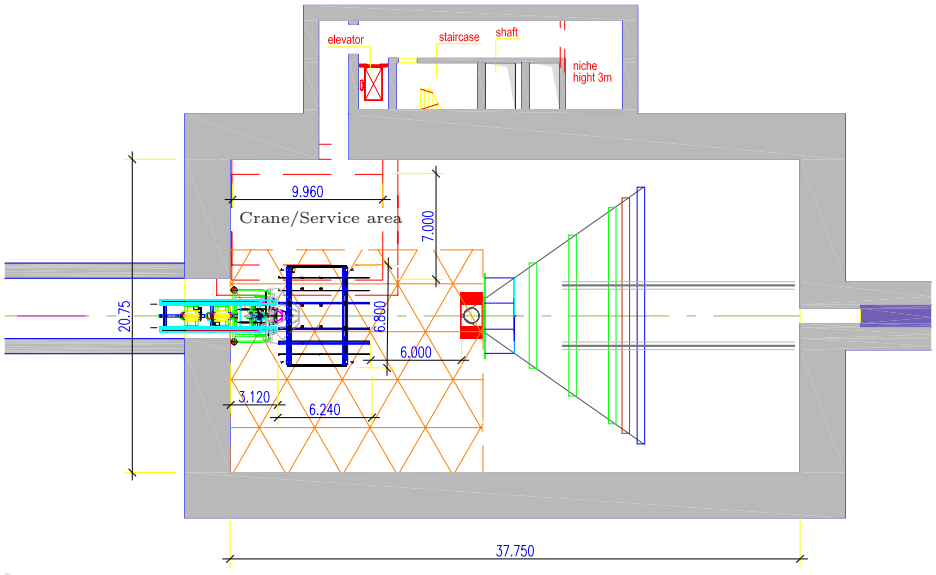

Fig. 19. Top view of the planned new HADES/CBM cave, showing the location of the HADES and CBM detectors, as well as the available service space.

space has of course to be shared between the two setups, HADES and CBM. At the current stage of cave design, the space allocated for HADES seems, however, to be sufficient. In order to shorten as much as possible the distance between HADES and CBM (for beam-optical reasons), the service area of HADES is now foreseen to be located underneath the access shaft (see Fig. 20, 19). The readout electronics of HADES and CBM will occupy a dedicated space below the HADES spectrometer. The floor area available will be of the order of 240 m^2, whereas for the HADES electronics about 25 m^2 is sufficient.

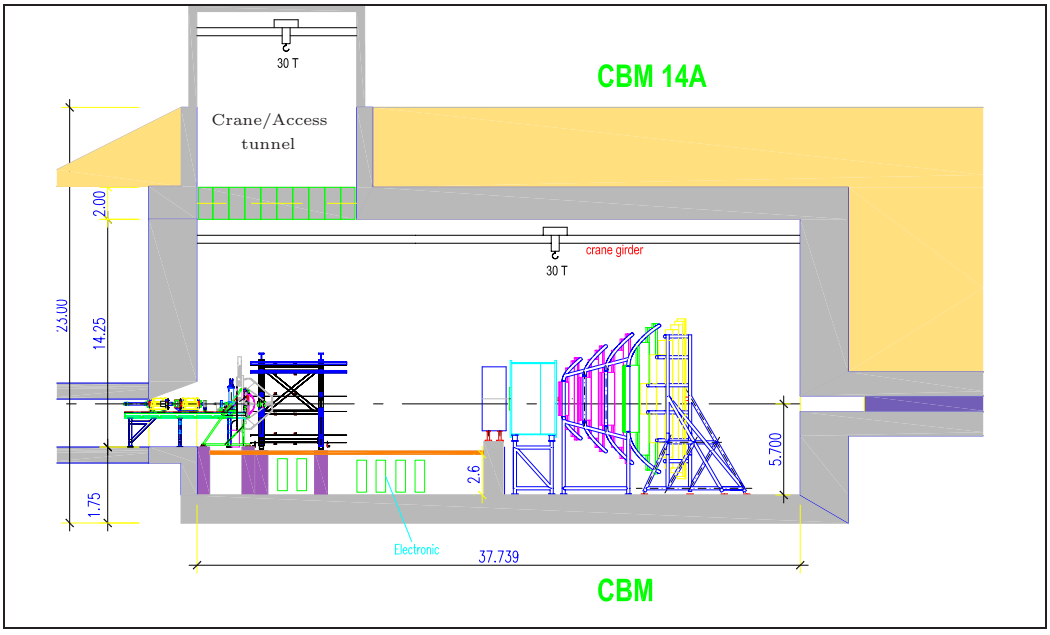

Fig. 20. Side view of the planned new HADES/CBM cave, showing the location of the HADES and CBM detectors, as well as the access shaft and cranes.

The distance between the focal points of HADES and CBM has to be kept as short as possible in order to avoid additional focusing magnets between the two target points. Although the beam line system is not yet fully designed at the current stage, the magnets located in front of HADES are expected to be sufficient for beam focusing for CBM as well. Such a solution simplifies significantly the beam line design.
The HADES/CBM cave will be located underground and a comfortable access to the cave via a pit is planned. As shown in Fig. 19 and Fig. 20, the access is planned to be located in the front part of the cave. A crane will be installed to lower the experimental equipment through the main access shaft. The size of the access hole to the cave has to be big enough to let pass the largest element of HADES, which is the magnet. Thus, the size of the access pit has to be at least $7\,\mathrm{m} \times 5\,\mathrm{m}$; the planned dimension of the pit is $7\mathrm{m} \times 9.9\mathrm{m}$. The capacity of both outer and inner cranes are designed to be 30 tons, which fulfills the HADES requirements. The weight of the heaviest elements of HADES, which currently is the magnet, is 5 tons. Taking into account the planned calorimeter for HADES, the minimal capacity of the shaft crane should not be less than 30 tons.

The experimental infrastructure includes not only the cave, but three additional rooms at ground surface level: a control room, a computer room and a service place for detectors. The main control room, from which the monitoring, recording and logging of the spectrometer parameters will be performed, should have a size of the order of $7\,\mathrm{m} \times 8\,\mathrm{m}$ and will be divided into 2 equal parts: a hardware part and a console part. The hardware part of the control system, consisting of the event-building computer system, the electronics for

trigger monitoring and configuration, like VME, CAMAC, NIM crates, etc., should be separated acoustically and thermally from the console part where the shift crew will operate the spectrometer. The control room has to be equipped with air-condition, separately for the hardware part and the console part in order to assure optimal working conditions for the equipment and a comfortable environment for the operating crew. At least five workplaces need to fit into this room in order to allow to operate the HADES spectrometer in all phases of a run. During the startup process up to five people are needed, but for normal operation two to three people are probably sufficient. The computer room will be of the same size as the main control room and will provide an appropriate number of terminals with network infrastructure, air conditioning, printers for the scientists participating in an experiment; 15 workstations are needed for this purpose. This room will also serve as a meeting room during experiments and tests as well, and thus will be equipped with a projector and conference equipment like loudspeaker and video camera. The detector service room is essential for any maintainance work and testing, and will be located close to the cave, below ground. Only maintenance and repairs are expected to be performed in this room; it will not serve as a long-term storage place. The space to be allocated for this room is 7 m×8 m. Standard infrastructure has to be provided: 3-4 terminals, network, printer and a number of 220 V power outlets.

4.3 Cave infrastructure (cooling water, power lines, air-conditioning)

Each subsystem of the spectrometer equipped with front-end electronics must receive sufficient incoming 220 V power to supply all installed components. Into the total power consumption of HADES in operation enter two main contributions: the detector part, which consists of the power supply for front-end electronics, event builders and HV supply for detectors, and the power supply of the magnet system. Whereas the total power consumption of detectors, including read-out systems, is estimated to be below 50 kW, the magnet system requires 150 kW, with 100 kW consumed by the cryogenic compressor alone. The compressor is part of the stand-alone cryogenic system of the HADES magnet and will not be needed in case the magnet can be supplied from the FAIR cryo infrastructure, thus reducing the needed power by 100 kW.

Based on the fact that all of the input power is released again as heat, the estimate for the cooling needs of the air conditioning in the cave is 50 kW. The cave cooling infrastructure consists of the following systems: a standard air-condition device, providing the required temperature and humidity of the air inside the cave, a dedicated MDC front-end electronic cooling device, assuring stable temperature of the MDC front-end cards, and a water cooling circuit used for VME, CAMAC and NIM crates. These three systems guarantee stable conditions during experiments.

4.4 Transfer of the spectrometer (disassembly, transport and installation)

The transfer of the HADES detection system with its whole infrastructure to the new location in the CBM cave will be performed in several steps. In a first step, all subsystems will be dismounted (sector wise) from the main frame and all disassembled pieces of the spectrometer will be stored in an adequate storage place (e.g. the roof of the present cave). In the next steps, the HADES main frame and the magnet will be transported to the new cave.

4.4.1 Disassembly

The dismounting of the HADES spectrometer will be started from the rear end. At first, the PreShower detector mounted together with the RPC on the sector frame will be removed from the main frame and transported to the storage area. Dismounting of the RPC detectors is not necessary. Per sector, a storage area of $3\,\mathrm{m} \times 2\,\mathrm{m}$ is needed, in total 36 m^2 should hence be available in the storage place.

The outer MDC system (2 outer planes) mounted together with the TOF on one support frame will next be dismounted from the main frame. The TOF and the outer MDC detectors will be taken apart and transported to the storage place separately. For those 12 parts of the spectrometer, 6 outer MDC sectors (6 x 3m x 5m = 90 m^2) and 6 TOF sectors (6 x 3m x 2m = 36 m^2) storage space in the order of 126 m^2 has to be reserved.

The inner MDC system will be transported and stored in two pieces, each layer of the MDC chambers mounted together on the support frustum. The required space for one MDC layer at the storage place is $4\ \mathrm{m} \times 4\ \mathrm{m} = 16\,\mathrm{m}^2$. A similar amount of storage space will be needed for the RICH detector. The removal of the RICH detector will be performed in one piece as well. The total amount of required storage place has to be in the order of $184\,\mathrm{m}^2$. In addition, $20\,\mathrm{m}^2$ must be foreseen for equipment needed at the storage place. As each of the subsystems mentioned has already been dismounted from the HADES main frame at least once, quite some experience is available and all disassembly/assembly procedures are well prepared, defined and tested.

Once the detectors and electronics have been disassembled and transported to the storage place, the remaining infrastructure (gas supply, HV cables, LV cables, power cables) will be taken apart from the main frame. The whole supply infrastructure currently installed in the HADES cave is planned to be reused, thus dismounting has to be performed with special care.

Next, the HADES main frame will be disassembled and transported to the new cave where it will immediately be reassembled and installed. Finally, the magnet will be disconnected from the old cooling infrastructure, prepared for

moving and transported directly from the present location to the new one.

4.4.2 The storage place

For the transfer of the whole HADES system to the new cave more than 6 months will be needed and thus a well-prepared storage place for detectors and parts has to be provided. Although the location is not yet decided, the most convenient area to be used for this purpose is the roof of the present HADES cave. During storage all subsystems based on wire chambers have to be flushed with nitrogen gas. In total, assuming the nitrogen supply per chamber to be in the order of 5 liters per hour, an amount of 210 liters of nitrogen per hour has to be provided. Stable temperature and low humidity of the air is crucial and has to be provided in order to avoid corrosion of the metal parts of the detectors and electronics. Thus, the storage place will be covered by a tight foil tent and equipped with an air conditioning system.

4.4.3 Installation

The installation procedure of HADES in the new cave will start with the main frame and will be followed by the installation of the magnet system. The magnet itself and the main frame will be put into the final position. Once they are in measurement positions, the connection between magnet and cryo plant will be established. At this stage a magnet alignment procedure should be performed. Both, the main frame, as well as the magnet system have to be aligned with respect to each other in order to assure proper momentum reconstruction of the spectrometer. It is currently under discussion what precision has to be achieved and what kind of alignment procedure can be used in order to guarantee useful results. One of the techniques which can be used for this purpose is photo-alignment [27], successfully used already for HADES subsystem alignment. This is presently considered to be a feasible solution, but it has to be proved that the method indeed is able to deliver the required precision.

As a next step, the supply infrastructure has to be installed and tested in the cave in order to provide a working environment for all detectors. At the same time, readout electronics and HV modules can be transported, together with all the cables, and installed underneath the main frame. Once the gas supply system, power supplies and readout electronics are installed, the subsystems RICH, TOF and PreShower can be transported from the storage place and be installed into the main frame. Each remounted subsystem will be connected to the needed supply lines and basic tests can be performed. At this stage of installation, additional alignment measurements may be usefull to provide input to the overall alignment procedure.

4.5 Magnet: transport, installation and cryo system

4.5.1 Transport

The magnet's dimension, weight and fragile components call for special attention and its transport is expected to be the most difficult action during the whole moving process of the spectrometer. The magnet dismounting process will start once all subsystems are located in the storage place. In a first step, the magnet will be disconnected from the cryo plant by dismounting the cryo transfer line. The magnet will be transported to the new cave in one piece.

4.5.2 Cooling: helium and nitrogen

According to the current stage of FAIR planning, the FAIR cryogenic system fits nicely the HADES magnet requirements. Thus, the simplest option would be to connect the magnet to the FAIR cryogenic helium supply infrastructure. The planned FAIR cryogenic system will deliver helium at 4.5 K and 50-80°K for shield cooling. The parameters of the supercritical helium fit our needs and only a slight modification of our system is required. Currently, we use liquid nitrogen for cooling of the shield of the HADES magnet. In the new cave, the use of liquid nitrogen is, however, not recommended for safety reasons and liquid nitrogen will not be provided by the FAIR cooling infrastructure. At first look, our magnet should be able to run with helium, as a cryogen for cooling of the shield of the HADES magnet, and this would require slight modifications of the system (some valves mainly). In case the FAIR cryo infrastructure is not available in the CBM cave region, the installation of the old HADES cryo system will be required and space needed for the old cryo system has to be provided.

4.5.3 Setup in the new cave

Due to the fact that the experts who built the magnet (magnet department of OXFORD INSTRUMENT company) are not available any more, major modifications of the mechanical construction of the system should be avoided. Thus the setup for the magnet in the new cave is planned to be organized in the same way as it was in the existing cave. This mainly concerns the valve box and the transfer line which provides cryogen transfer between the valve box and the magnet itself.

4.6 Commissioning of the whole system

The performance of the fully installed system has to be demonstrated experimentally and therefore the first experimental run should start with light collision systems. The most useful experiment which can help in proving that the spectrometer is ready and operational is an elastic p+p scattering measurement. This reaction channel will allow for checking the hardware (detectors, trigger system, data acquisition), software, as well as the analysis part, like event building, momentum reconstruction and alignment. Experience tells

that an extremely important issue for high resolution spectroscopy is the perfect understanding of the alignment and this will be the main goal of the first experimental run. The duration of such a run is expected to be close to one week.

5 Cost estimations and time schedule

5.1 Time Schedule

According to the current planning of the FAIR facility the installation and test phase of SIS 100 synchrotron is planned in the period: 2012 - 2014 and can change in the future. In addition the date of the shutdown of the SIS18 is not fixed. The start time of the transfer of the HADES spectrometer will happened after the shutdown of the SIS18 and thus in the time table the shutdown of the SIS18 is used as a beginning of the transfer process.
The availability of manpower used during the planning assumes an Full-Time Equivalent (FTE) of 5.0 assigned to the project from which an FTE of 1.0, cryo expert, has to prepare the transport of the magnet.
According to the proposed time schedule the transfer of the HADES spectrometer to the new cave should take about 12 months. Then about 6 months can be allocated for the further tests (like cosmic run, alignment) and for the commissioning phase which can be started once SIS100 and the beam line to the CBM/HADES cave are ready.

5.2 Cost estimation

The cost estimates for the individual phases and components are quoted in the table below, the manpower cost (an FTE of 5.0) is not included. The Most of the old infrastructure like power lines, gas lines, detector frames will be reused in the new cave in order to not only lower the costs but also to significantly reduce the manpower involvement in the process.

		← shutdown of the SIS18				
Project / subproject / item	**duration**	**I-III**	**IV-VI**	**VII-IX**	**X-XII**	**XIII-XV**
Cave preparation	**6 month**					
Control room	1 month					
Computer room	1 month					
Service place for detectors	1 month					
Cooling infrastructure	3 months					
Air-conditions	3 months					
Power lines	3 months					
Beam line	13 months					
HADES transfer						
HADES disassembling	**6 months**					
Transport to the storage place	6 months					
Old supply lines disassembly	6 months					
Storage place	**1 month**					
N2 gas, vinyl pipes	1 month					
Foil tent	1 month					
Support fames for detectors	1 month					
Transport / installation in the new cave	**6 months**					
Mainframe transport/installation	1 month					
Supply lines installation	3 months					
Transport/installation of subsystems	6 months					
Magnet / beam line/ main frame alignment	1 month					
Magnet	3 months					
Preparation for transport	1 months					
Transport	2 weeks					
Installation	2 weeks					
Cryo supply	3 months					

Table 5
Time table.

Project / subproject / item	**cost**	**remarks**
Cave design		
Control room	90,000.00 €	Separate room for HADES
Computer room (equipment only)	10,000.00 €	Shared with CBM, equipment only
Service room for detectors (equipment only)	10,000.00 €	Shared with CBM, equipment only
Cooling infrastructure in cave	130,000.00 €	Water cooling
Air-condition in control room	30,000.00 €	
Power lines in cave and control room	120,000.00 €	
Beam line	130,000.00 €	Beam focus on HADES target
HADES transfer		
HADES disassembly	0.00 €	
Storage place		
N2 gas, vinyl pipes	15,000.00 €	
Foil tent	5,000.00 €	
Support fames for detectors	25,000.00 €	
Transport / installation in the new cave		
Transport (mainframe, subsystems)	50,000.00 €	
Installation of subsystems	20,000.00 €	
Magnet / beam line/ main frame alignment	50,000.00 €	
Magnet		
Preparation for transport	15,000.00 €	
Transport	20,000.00 €	
Installation	50,000.00 €	
Cryogenic distribution system	150,000.00 €	FAIR cryo plant will be used
TOTAL	**920,000.00 €**	

Table 6
Cost table.

References

[1] P. Braun-Munzinger, J. Stachel, Nucl. Phys. A638, 3c (1998).

[2] G. Agakichiev et al. Physical Review Letters 98 (2007)052302

[3] G. Agakichiev et al. Physics Letter B 663 (2008) 43-48

[4] D. Adamova et al. [CERES Collaboration], submited to Phys. Lett. B, nucl-ex/0611022

[5] R. Arnaldi et al. [NA60 Collaboration], Phys. Rev. Lett. 96, 162302 (2006).

[6] A. Andronic, priviate communication and NPA 772 (2006) 167.

[7] PRC 73 (2006) 034905.

[8] J.Cleymans, J.Randrup, Phys. Rev. C74 (2006) 047901.

[9] H. Oeschler et al. nucl-th/070180.

[10] R.Rapp, J.Wambach, Adv. Nucl. Phys. 25,1, (2000).

[11] W. Kuhn, Nuclear Physics A 583 (1995) 607–616

[12] P. Fonte, A. Smirnitski and M.C.S. Williams, Nucl. Instr. and Meth. A 443 (2000) 201.

[13] J.L. Klay et al. Phys. Rev. C68 (2003) 054905.

[14] D. Schumacher, S. Vogel, and M. Bleicher, nucl-th/0608041.

[15] A. Kugler et al., Proceedings of XLIV International Winter Meeting on Nuclear Physics, Bormio 2006, p.282

[16] A. Balanda et al., Nucl. Instr. and Meth. A 351 (2004) 445.

[17] M. Sanchez, *"Kick Plane"*, Internal Hades Report, GSI 2000

[18] Hades et al., arXiv:0902.3478.

[19] D. Belver *et al.*, Nucl. Phys. Proc. Suppl. **158**, 47 (2006);

[20] H. Alvarez-Pol *et al.*, Nucl. Instrum. Meth. A **535**, 277 (2004).

[21] M. Weber, Diploma thesis, TU München 2007.

[22] M. Traxler *et al.*, GSI Scientific Report 2005, (GSI Report 2006-1).

[23] M. Traxler *et al.*, GSI Scientific Report 2006, (GSI Report 2007-1).

[24] Lustre is a scalable, secure, robust, highly-available cluster file system http://wiki.lustre.org

[25] I. Froehlich *et al.*, IEEE Transactions on Nuclear Science, vol. 55 (2008) 59-66, 2008.

[26] ETRAX, AXIS Communications, Sweden
http://www.axis.com/products/dev/product_list.htm

[27] http://www.photomodeler.com/

Contents